COVER SHEET

Paper Number: **403**

Title: **Integration of multi-scale modeling of composites under high strain rate impact with surrogate**

Authors: Shu Shang
         Nam H. Kim
         Minhyung Lee

ABSTRACT

This paper presents multiscale modeling of composites under high strain rate impact using surrogate models. The material response under high strain rate impact has relatively been well studied for metallic materials. However, when it comes to composites, the mathematical model for failure becomes very complicated due to various failure modes. Under high strain rate impact, the major failure mechanisms are fiber breakage, fiber debonding and pullout and delamination between adjacent plies. The first two mechanisms initiate at the fiber-matrix level and should be modeled in micro-scale, while delamination should be modeled in meso-scale and macro-scale. In micro-scale, fiber-matrix structure is modeled to simulate fiber fracture and debonding, which contribute to the degradation of material properties in macro-scale. In macro-scale, high strain rate impact is simulated using nonlinear explicit finite element analysis with the degraded material properties from micro-scale simulation. Delamination is also included in macro-scale.

This paper develops a multiscale modeling technique of fracture failure behavior of composites under high strain rate. Multiscale modeling of fracture phenomena of composites will consist of (1) micro-scale modeling of fiber-matrix structure using the unit-volume-element technique, which can incorporate with the boundary effect, and the level set method for crack modeling, which can model the crack propagation independent of finite element mesh; (2) macro-scale simulation of composite panels under high strain-rate impact using material response calculated from micro-scale modeling; and (3) surrogate modeling to integrate the two scales. The degradation of material strength due to fiber cleavage will be calculated from micro-scale modeling and will be used in macro-scale simulation. The surrogate model includes both micro-scale parameters, such as volume fraction, and macro-scale parameters, such as strain rate. The proposed multiscale modeling technique can provide a practical alternative to massive parallel processing.
Keywords: multi-scale modeling, high strain rate, surrogate

_____

Nam H. Kim, Associate Professor, Dept. of Mechanical & Aerospace Engineering, College of Engineering, University of Florida, USA
Minhyung Lee, Professor, School of Mechanical & Aerospace Engineering, Sejong University, South Korea
Shu Shang, Graduate Research Assistant, Dept. of Mechanical & Aerospace Engineering, College of Engineering, University of Florida, USA

INTRODUCTION

Composite materials are gaining increasing prominence in engineering applications. They allow to take advantage of different properties of component materials, of the layup configuration and of the interaction between the constituents to obtain a tailored behavior. Composite materials may present high stiffness and damping, improved strength and toughness, improved thermal conductivity and electrical permittivity, improved permeability, and unusual physical properties such as negative Poisson's ratio and negative stiffness inclusions [1].

For most of linear analyses of composite structures, instead of taking the individual constituent property and geometrical distribution into consideration, homogenized material properties are used. However, when higher accuracy is required, we need to refer directly to the microscopic scale. Then multi-scale modeling is needed to couple macroscopic and microscopic models to take advantage of the efficiency of macroscopic models and the accuracy of the microscopic models [2].

Most composite materials are multi-scale in nature, i.e. the scale of the constituents is of lower order than the scale of the structure. The length scales range from the fiber size whose dimension is measured in microns, to the individual plies in laminates whose thicknesses are measured in fractions of millimeters, to the laminates themselves whose sizes are measured in millimeters. The laminates then form parts of composite structures whose sizes are measured in meters. The physical phenomena observed at any of these length scales are linked to those on the neighboring length scales.

For fiber-reinforced composites, the overall hierarchy of multi-scale analysis is composed of micro-level (fibers and matrix), meso-level (plies) and macro-level (laminated composite). One of the major challenges is how to bridge the scales. Currently, typical multi-scale modeling techniques use parallel processing to couple the scales. However, this requires huge computational resources. Bridging three or more scales often necessitates unrealistic computing power even with the most versatile facilities available. Another situation is uncertainty quantification often requires numerous repetitions of response analyses, and it is easy to lose the feasibility of such huge computational resources.

A new bridging methodology is proposed to overcome the computational burden in typical multi-scale modeling techniques, which often require massive parallel processing. The constitutive relations at a macroscopic point are estimated by performing micro-scale finite element analysis on a unit volume element. Two major failure modes, fiber breakage and fiber debonding, both initiate at the fiber-matrix level and contribute to material property degradation, are modeled in the micro-scale. And delamination between plies should be modeled in meso-scale and macro-scale. Then the two hierarchy of multi-scale analysis are integrated using surrogate modeling. This procedure can be regarded as sequential multi-scale modeling, in which the micro-to-macro homogenization process is made separately from the structural analysis. However, in typical sequential multi-scale procedure, micro-scale modeling is used to estimate the parameters of a certain material model. Only limited information can be transferred from micro-scale to macro-scale because of the limitation of material models. Compared with homogenization technique used in typical sequential multi-scale procedures, we expect the proposed

bridging methodology based on surrogate modeling to be able to transfer more information from the micro-scale to the macro-scale.

UVE APPROACH FOR MODELING FIBER FRACTURE AND PULLOUT

Unit Volume Element

A variety of theories have been developed for micro-scale modeling of composite materials analytically, such as effective medium models of Eshelby [3], Hashin [4] and Mori and Tanaka [5]. And the traditional numerical method is representative volume element (RVE). A typical RVE of unidirectional fiber-reinforced composites is shown in figure 1. The analytical methods ignore the interaction among fibers by assuming that fiber is relatively small. This is not accurate since the nominal volume fraction of fiber is between 0.5 and 0.7, there exists a strong interaction between fibers. RVE assumes the periodic characteristics of fiber composites and applies the periodic boundary condition. However, when it comes to uncertainty quantification, RVE becomes inappropriate since periodicity in RVE works against fiber fracture and uncertainty in the layout of fibers. Uncertainty is caused by randomly distributed distance between fiber, but the periodicity enforces the distance in a certain pattern. In addition, the periodic boundary condition can often be inappropriate for composite plates. The dimensions in the membrane plane are large enough to be considered periodic, but the thickness direction of composite plates is relatively small, and the boundary effect becomes important in the response. In this research, instead of RVE, the unit volume element (UVE) is used. The major different between RVE and UVE is the boundary condition. UVE does not have periodic boundary condition in the thickness direction.
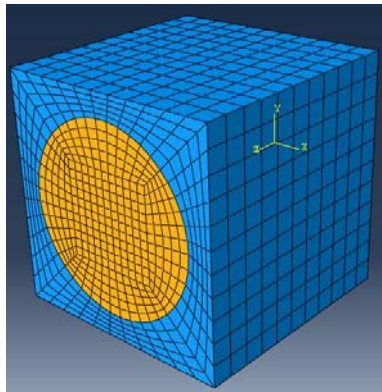

Figure 1. Structure of RVE of unidirectional fiber-reinforced composites.

SIZE OF HETEROGENEOUS STRUCTURE

The appropriate size of the heterogeneous structure should be decided first because the material behavior of the element placed at the most outer area would be different from the behavior of the one placed in the middle of the structure.
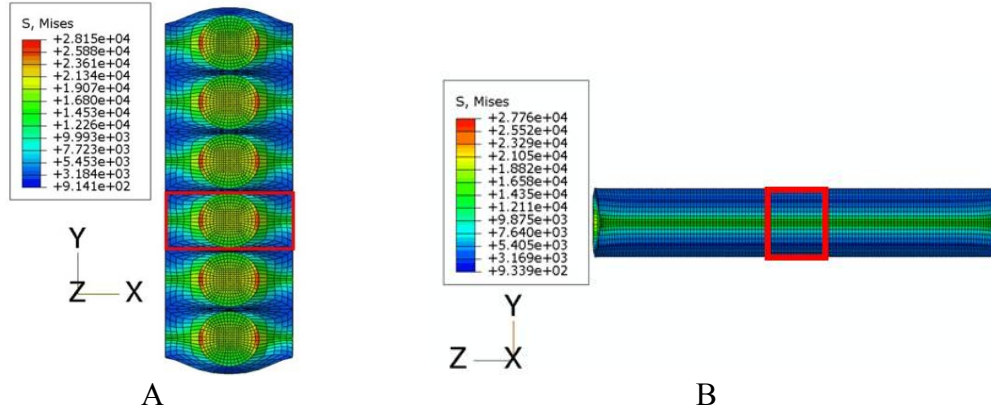
Figure 2. Heterogeneous structure composed of UVE piled up. A) Y direction. B) Z direction.

Figure 2 shows the deformed shape of the structures composed of several fibers in y direction and z direction under x direction displacement loading respectively [6]. Jinuk Kim [6] found out that three UVEs in y direction and z direction should be enough for the size of the heterogeneous structure by comparing the effective stress in UVEs at different position. The heterogeneous structure model in this research is shown in figure 3.
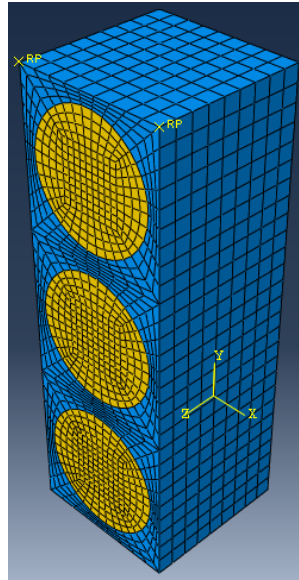

Figure 3. Heterogeneous structure model.

BOUNDARY CONDITIONS

The dimensions in x and z directions, that are transverse direction and longitudinal direction, are large enough to be considered periodic. And periodic boundary conditions will be imposed on the surfaces perpendicular to x axis and y axis. The periodic boundary condition constrains the boundary to keep the relative displacement constant according to the strain on that boundary. It can be expressed as follows:

$$u_i(x_0 + d) = u_i(x_0) + \bar{\varepsilon}_{ij}d_j \tag{1}$$

where $\bar{\varepsilon}_{ij}$ is the average strain component and d is the characteristic distance.

Besides the periodic boundary condition, other boundary conditions are needed to remove rigid body motion of the structure. And symmetric boundary condition is applied to the bottom surface.

AVERAGE STRESS VALUES

The average scheme is used to calculate representative stress values of the UVE,

$$\overline{\sigma}_{ij} = \frac{1}{V}\int_V \sigma_{ij} dV \tag{2}$$

where σ_{ij} is the local stresses in the UVE or micro stresses.

As UVE itself is composed of small elements, the average can be achieved by integrating individual elements. In order to perform volume integral of each element, the Gaussian integration method is applied

$$\overline{\sigma}_{ij} = \frac{1}{V}\sum_{i=1}^{NE}\int_V \sigma_{ij} dV_i = \frac{1}{V}\sum_{i=1}^{NE}\sum_{k=1}^{8}\frac{(\sigma_{ij})_k}{8}V_{ik} \tag{3}$$

where NE is the number of element, V_{ik} is the volume of an integration point of an element.

Since the material behavior of UVE placed at the most outer area would be different from the behavior of the one placed in the middle of the structure, average stress of inner part of the structure will be calculated, as shown in figure 4.
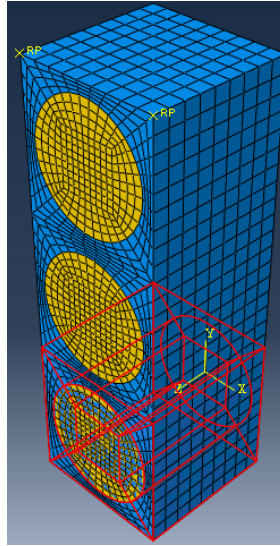

Figure 4. Inner part of heterogeneous structure.

Modeling of major damage modes

Under high strain rate loading, the major failure mechanisms are fiber breakage, fiber debonding and pullout and delamination. Figure 5 shows the major failure modes observed in actual experiments. From this figure, we can see that fiber breakage and debonding both initiate and can be observed in the micro scale and will be modeled in the UVE. However, delamination between plies, though associated with matrix cracking initiated from the micro scale, is observed in the

meso scale and thus will not be modeled in the unit cell. And the modeling of debonding will be considered in further study.

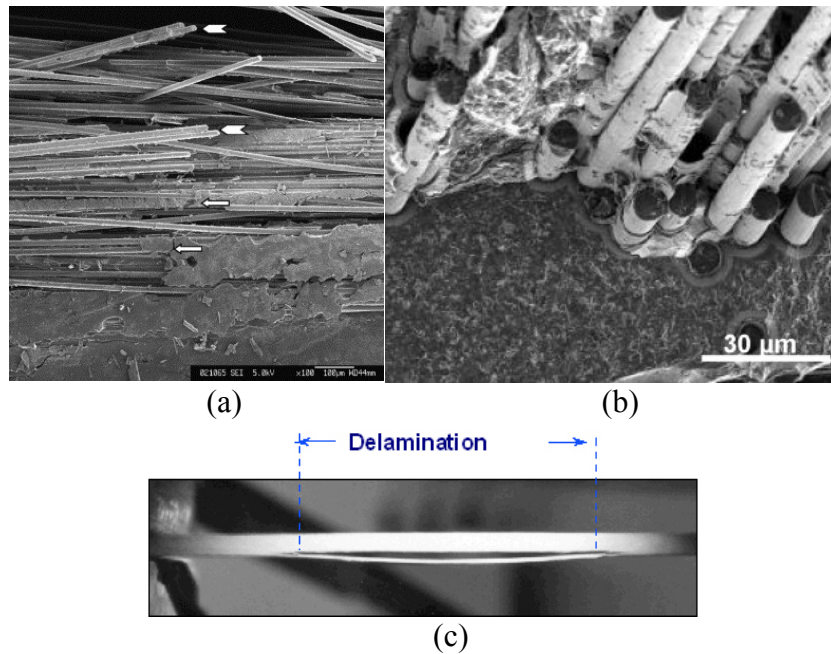(a)   (b)

(c)

Figure 5. Major failure modes under high strain rate impact: (a) fiber breakage; (b) fiber debonding and pullout; (c) delamination.

MODELING OF FIBER FRACTURE

Fiber carries most of the load and thus fiber fracture contributes most to the degradation of material properties. In this research, the crack in the fiber is modeled as enriched feature of finite elements. The extended finite element method (XFEM) uses the enriched feature and is an extension of general FEM allowing the discontinuities to exist in an element by enriching degrees of freedom with special displacement functions. This method is efficient especially when crack propagation is to be investigated since it does not require remeshing as fracture of fiber progresses.

Under high strain rate impact, fiber behaves as brittle material and fiber fracture occurs completely in an extremely short time period. Figure 6 shows the stress-strain curve of a common carbon fiber T300 under different strain rates [7]. We can see that the curve is composed of elastic region and sudden fracture. And since the degradation due to fiber fracture is the focus, the propagation of the crack is not considered. Stationary crack can be defined using an enrichment command and assigning crack domain in Abaqus. When the elements are intersected by the defined stationary crack domain, the elastic strength of that element is regarded as zero, which can be regarded as discontinuous. Figure 7 shows the assignment of a stationary crack and the stress field near the crack front [6].
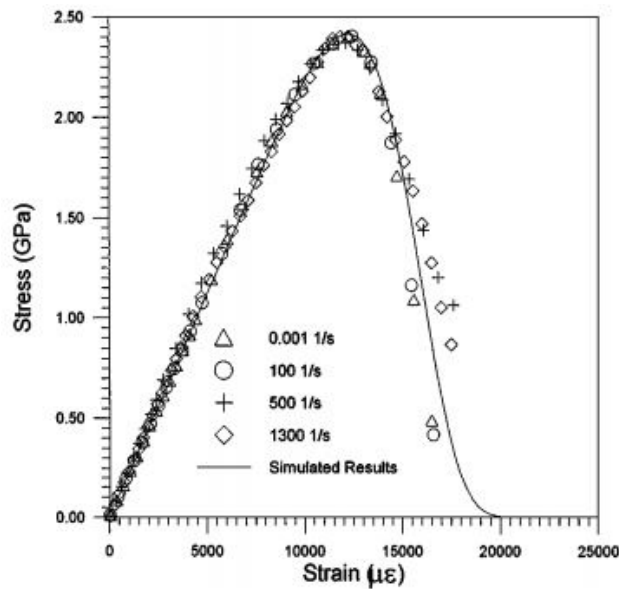
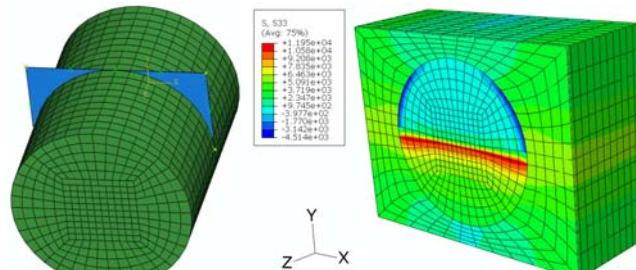Figure 6. Stress-strain curve of T300 under different strain rates.

Figure 7. Transverse direction crack in fiber.

Strain Rate Effect on Material Property

As mentioned earlier, this research focuses on a high strain rate impact phenomenon. Strain rate might have a big effect on the material response. High strain rates tend to favor the elastic properties of materials. Elasticity is associated with load-bearing performance as embodied in properties such as strength and stiffness. However, low strain rates favor the viscous or energy-damping aspects of material behavior. Viscous flow is associated with energy management, often referred to as impact resistance or toughness.

For composite materials, fibers are the main load-bearing elements and reliable information of the properties of fibers under high strain rate loading is important. Because of technical difficulties in tests, currently, it is difficult to obtain the dynamic properties of a single fiber directly. Chi et al. [8] proposed an approach for determining the static properties of single fiber by measuring those of fiber bundles. Xia et al. [9] extended the method to dynamic state and first successfully performed tensile impact tests on fiber bundles. Their testing strain rate was up to 1100/s. One of the most popular types is carbon fiber. Table 1 shows mechanical properties of two common carbon fibers, T300 and M40J, at different strain rates [10]. It can be observed that for these two kinds of carbon fibers the effect of strain rate on

material property can be ignorable. However, for other kinds of fibers, the effect of strain rate might be very prominent. Figure 8 shows the relationship between strain rate and the ultimate strength of M40J, T300, E-glass and Kevlar49 fiber bundles [10]. It can be concluded that M40J and T300 are strain rate insensitive materials while E-glass and Kevlar49 are sensitive to strain rate.

TABLE I. Mechanical properties of T300 and M40J at different strain rates.

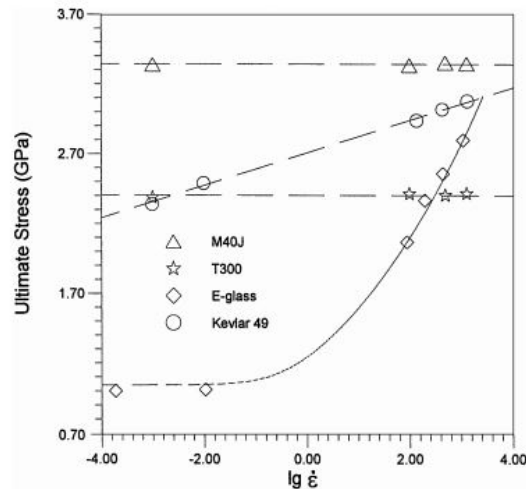| $\dot{\varepsilon}$ (s^{-1})	E (GPa)	$|\Delta E/E|$	ε_b (100%)	$|\Delta\varepsilon_b/\varepsilon_b|$	σ_b (GPa)	$|\Delta\sigma_b/\sigma_b|$
0.001	357.9	2.3%	1.26	4.1%	3.339	3.2%
100	359.6	2.5%	1.28	2.2%	3.336	2.6%
500	360.1	2.0%	1.29	2.3%	3.354	1.2%
1300	359.1	2.1%	1.29	3.4%	3.347	2.6%
Average value	359.2	---	1.28	---	3.344	---
0.001	223.2	4.5%	1.35	4.1%	2.387	3.6%
100	227.4	3.7%	1.32	4.0%	2.415	3.2%
500	223.5	3.4%	1.34	3.6%	2.404	2.8%
1300	225.6	4.1%	1.34	3.7%	2.418	3.4%
Average value	224.9	---	1.34	---	2.406	---

Figure 8. Effect of strain rate on ultimate strength of fiber bundles.

The matrix phase for fiber reinforced composites can be a metal, polymer or ceramic. Generally, the matrix works as binding materials that supports and protects fibers. And metals and polymers are usually used as a matrix because of ductility. However, under high strain rate impact, ductile materials tend to behave as a brittle material. Figure 9 shows experimental tensile stress-strain curves for PR520 resin, which is commonly used as a matrix, at different strain rates [11]. This figure indicates that as strain rate increases, ductility tends to vanish.
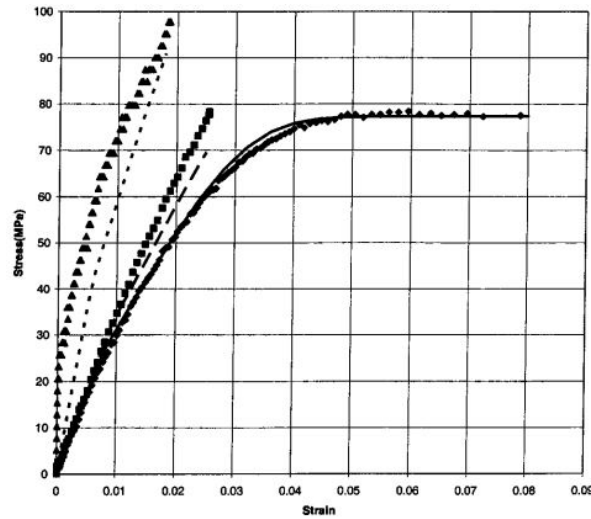
Figure 9. Experimental tensile stress-strain curves for PR520 resin at strain rates of 5x10-5/s (low rate), 1.4/s (medium rate) and 510/s (high rate).

For both fiber and matrix, linear elastic model will be used for simplicity. As mentioned in previous section, fracture of fiber will be modeled using extended finite element method. Damage and fracture of matrix is not the focus here since fiber is the main load-bearing element.

SURROGATE MODELING OF COMPOSITES CONSTITUTIVE RESPONSE

Kriging Surrogate

In this research, we propose to integrate micro-scale simulation with macro-scale phenomena with a surrogate modeling technique. As one of the most popular surrogates, kriging is used to estimate the behavior of the micro-structure. In addition, the surrogate can also be used to estimate uncertainty in micro-structure.

MODELING AND PREDICTION

Following [12], we adopt a model that treats the deterministic response y(x) as a realization of a random function (stochastic process) and a regression model,

$$\hat{y}(x) = \sum_{j=1}^{k} \beta_j f_j(x) + Z(x) \tag{4}$$

The random process Z(x) is assumed to have mean zero and covariance

$$V(w, x) = \sigma^2 R(\theta, w, x) \tag{5}$$

between Z(w) and Z(x), where σ^2 is the process variance and $R(\theta, w, x)$ is the correlation model with parameter θ.

The common functions $f_j(x)$ used in regression model are polynomial with orders 0, 1 and 2. And the most popular correlation function is Gaussian correlation function which takes the form

$$R(\theta, \mathrm{w}, \mathrm{x}) = \prod_{j=1}^{n} \exp[-\theta_j (\mathrm{w}_j - \mathrm{x}_j)^2] \qquad (6)$$

The optimal coefficients θ of the correlation function can be found by solving

$$\min(\det R)^{1/n} \sigma^2 \qquad (7)$$

DESIGN OF EXPERIMENTS

Experimental design is important since it decides how to select the inputs at which to run the analysis in order to most efficiently reduce the statistical uncertainty of the prediction. Latin hypercube sampling (LHS) will be used here.

Latin hypercube sampling, due to McKay et al. [13], is a statistical method for generating random samples from a multidimensional distribution ensuring that all portion of the design space is represented. Consider the case where we wish to sample m points in the n dimensional space. The Latin hypercube sampling strategy can be explained as follows:

Divide the interval of each dimension into m non-overlapping intervals having equal probability (e.g. for uniform distribution, the intervals should have equal size).

Sample randomly from the distribution a point in each interval in each dimension.

Pair randomly (equal likely combinations) the point from each dimension.

ACCURACY OF SURROGATE MODELING

Accuracy of surrogate is crucial here since it determines how accurate the information from micro-scale is transferred to macro-scale. One common measure of accuracy of surrogate is the predicted residual sum of squares (PRESS) statistic. A fitted model having been produced, each observation in turn is removed and the model is refitted using the remaining observations. The out-of-sample predicted value is calculated for the omitted observation in each case, and the PRESS statistic is calculated as the sum of the squares of all the resulting prediction errors:

$$PRESS = \sum_{i=1}^{n} \left(y_i - \hat{y}_{i,-i} \right)^2 \qquad (8)$$

With 280 data points, a kriging surrogate was fitted for each stress component. In this case, only elastic property is considered. And table II shows the PRESS error of each surrogate. The low value of PRESS errors indicates the high accuracy of the surrogates.

TABLE II. PRESS error of surrogate

Surrogates	σ_{11}	σ_{22}	σ_{33}	σ_{12}	σ_{13}	σ_{23}
Mean value/MPa	443.4256	443.3342	917.9036	215.8546	199.835	56.1257
PRESS error	0.0089	0.0055	0.0158	0.0022	0.0029	0.0006

Surrogate Modeling

As mentioned earlier, we use Latin hypercube sampling strategy to generate different combinations of strain components at which to run the simulation in Abaqus and calculate the average stresses. In Abaqus, in order to apply random

strain values, equation constraint is used in python script to control translational degrees of freedom of all the nodes on the boundary.

With strain values as input and stress values as output, we can construct a kriging surrogate for each stress component. This can be done using a Matlab kriging toolbox DACE [14]. Previously we have already mentioned that crack propagation in the fiber is not going to be investigated, only the degradation due to fiber fracture is the focus. We will have two UVE models with intact fiber and totally fractured fiber respectively, thus for each stress component two kriging surrogate will be constructed. Now, we need a criterion to determine when given certain strain values as input which UVE model should be called, i.e. we need a criterion to determine when fiber fracture happens. First we assume that axial stress, which leads to fiber fracture, is determined by axial strain only. To verify the accuracy of this assumption, we use LHS to generate samples of input, run the analysis, calculate the average stress and project all points on $\varepsilon_{33}/\sigma_{33}$ plane. Here, 3 stands for the axial direction. Figure 10 shows the data points and linear regression. However, it is clear that the error is not ignorable. The RMS error is 100.3, 10.93% of the average value of σ_{33}. Notice that when ε_{33} is zero, the value of the fitted linear function is about 250, which means that we cannot ignore the contribution of other strain components to axial stress.
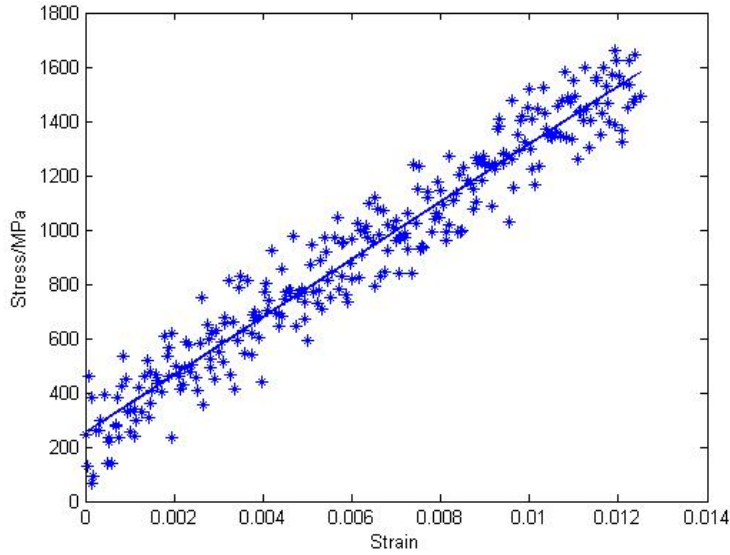

Figure 10. $\varepsilon_{33}/\sigma_{33}$ data points and linear regression.

Taking Poisson's effect into consideration, instead of using ε_{33} directly, we should use an equivalent $\overline{\varepsilon}_{33}$,

$$\overline{\varepsilon}_{33} = v_{13}\varepsilon_{11} + v_{23}\varepsilon_{22} + \varepsilon_{33} \tag{9}$$

where v_{13} and v_{23} are effective Poisson's ratios obtained from homogenization of elastic behaviors. Now project all points on $\overline{\varepsilon}_{33}/\sigma_{33}$ plane. Figure 11 shows the modified data points and linear regression.
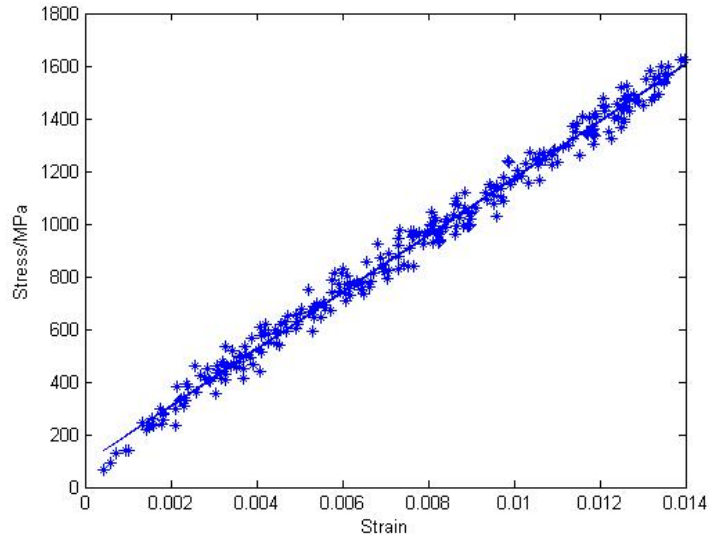
Figure 11. $\overline{\varepsilon}_{33}$ / σ_{33} data points and linear regression.

With $\overline{\varepsilon}_{33}$, the RMS error reduces to 40.857, 4.45% of the average value of $\overline{\sigma}_{33}$. And when $\overline{\varepsilon}_{33} = 0$, the value of the linear function is about 91MPa. It is accurate enough to use the equivalent axial strain as the fiber fracture criterion. By comparing $\overline{\varepsilon}_{33}$ with a certain critical value, we can decide which UVE model should be called so that all the inputs can be divided into two groups and two kriging surrogates can be constructed for each stress component.

MULTI-SCALE MODELING OF HIGH STRAIN RATE COMPOSITES RESPONSE

A composite panel is composed of many laminates with different fiber orientations. And a laminate is composed of many fibers through the thickness. A significant gap exists between the size of initiating fracture and the size of design interest, thus how to propagate information in micro scale to macro scale is a critical issue. As mentioned earlier, in this research, instead of massive parallel processing, we propose to use surrogate modeling to bridge micro-scale simulation and structural scale simulation to overcome the computational burden.
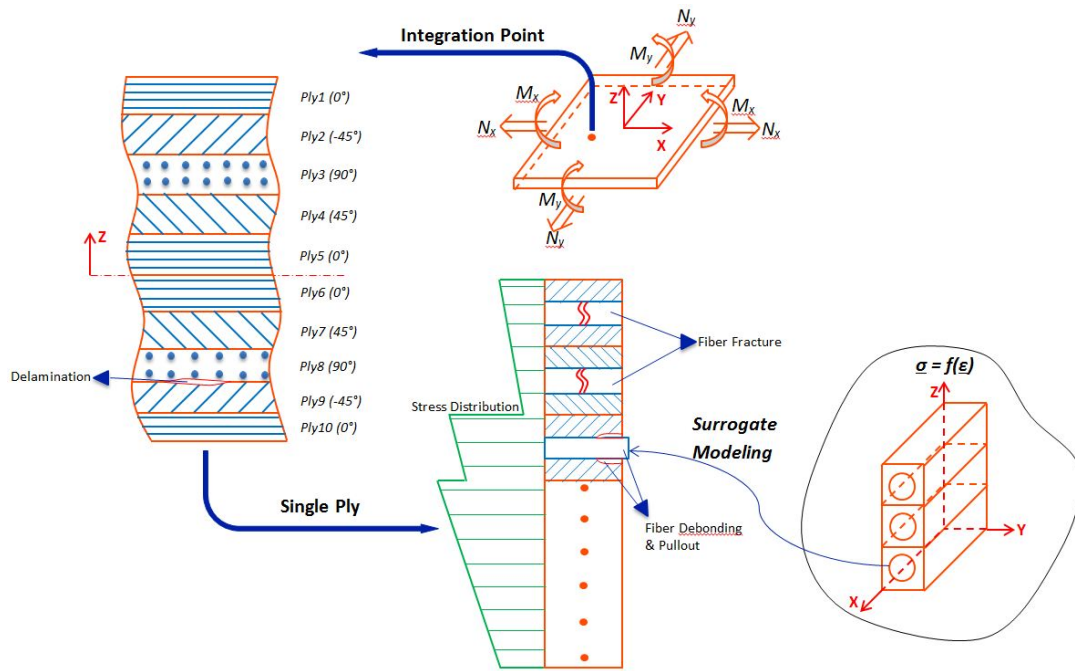
Integration Point

N_y

M_y

M_x

N_x

M_x

N_x

M_y

N_y

Z Y X

Ply1 (0°)
Ply2 (-45°)
Ply3 (90°)
Ply4 (45°)
Ply5 (0°)
Ply6 (0°)
Ply7 (45°)
Ply8 (90°)
Ply9 (-45°)
Ply10 (0°)

Z

Delamination

Single Ply

Stress Distribution

Fiber Fracture

Fiber Debonding & Pullout

Surrogate Modeling

$\underline{\sigma} = f(\varepsilon)$

Z Y X

Figure 12. Illustration of multi-scale modeling.

The basic idea of multi-scale modeling is illustrated in figure 12, in which a composite panel is decomposed into three levels: composite panel, ply, and fiber-matrix cell. In the composite panel level, the material behaves similar to anisotropic material. In this scale, finite element analysis is often used to simulate the global response of composite panel, which requires calculating stresses at integration points of each element. It is possible that some fibers are broken and debonding may occur between a fiber and matrix. The macro-scale stress calculation should include all these effects. Therefore, the multi-scale modeling is performed at each Gauss point of the FE mesh of the overall structure.

In the ply level, different directions of ply stacking sequence are considered in calculating the distribution of stress along the thickness direction. In this paper, 10 plies with lay-up configuration [0/-45/90/45/0]$_s$ are used. Strain calculated in the panel level is converted to strain at each ply. The strain at different locations of a ply is then sent to fiber-matrix cell level to calculate stress at that location. Since the fiber direction changes at different plies, coordinate transformation must be performed to convert strains and resulting stresses between the local and global coordinate system. Also notice that delamination between plies initiates in this scale. However, this failure mode is not covered since the focus of current work is micro-scale modeling and propagating information in the micro-scale to macro-scale using surrogate modeling technique.

In the fiber-matrix level, fiber and matrix phases are modeled separately. Two major failure modes, fiber fracture and fiber debonding, are considered. Fiber fracture is modeled using extended finite element method. The interfacial property between fiber and matrix is crucial here. However, it is difficult to obtain this property through experiments. In this scale, with strain values sent from higher level, UVE approach is used to calculate effective stresses. Instead of massive parallel processing, kriging surrogate is constructed with strain inputs generated from LHS sampling and stress outputs calculated from UVE model analyzed in

Abaqus. The multi-scale surrogate modeling technique proposed here can overcome the computational burden in typical multi-scale modeling technique and provide feasibility to uncertainty analysis based on large amount of repetition of response analysis in future research.

NUMERICAL STUDY AND VERIFICATION

Verification of this framework is done by conducting single element tensile test in a commercial explicit finite element program ls-dyna. The verification is achieved by comparing the behavior of the user-defined material developed from surrogate modeling with the behavior of a composite material model MAT22 in ls-dyna with parameters calculated from homogenization technique.

In this study, the constituents of the composite material are e-glass fiber and epoxy resin. Their elastic properties are listed in table II.

TABLE III. Elastic properties of fiber and matrix

Elastic properties	Stiffness/MPa	Poisson's ratio
E-glass	81,000	0.22
Epoxy	3,000	0.398

First, let's consider linear elastic case, that is to treat both fiber and matrix as linear elastic material. Homogenized properties are obtained for RVE and UVE, respectively. Figure 13 shows the comparison of material behavior in both longitudinal and transverse directions for elastic case. Here, the UMAT45 refers to the user-defined material model. As we can observe from the comparison of stress/strain curves, the surrogate based material model UMAT45 shows good accuracy and agrees well with the composite material model MAT22.

Now let's move to elastoplastic case. E-glass fiber is still treated as linear elastic material. Plasticity of epoxy is considered. Figure 14 shows the stress/strain curve of epoxy from tensile test and the approximate behavior to be implemented in Abaqus. Figure 15 shows the comparison of material behavior in both longitudinal and transverse directions for elastoplastic case. In longitudinal direction, most of the load is carried by the fiber, so the introduction of matrix plasticity has almost no influence on the material behavior. In transverse direction, discrepancy between the curves shows up around 0.17%.
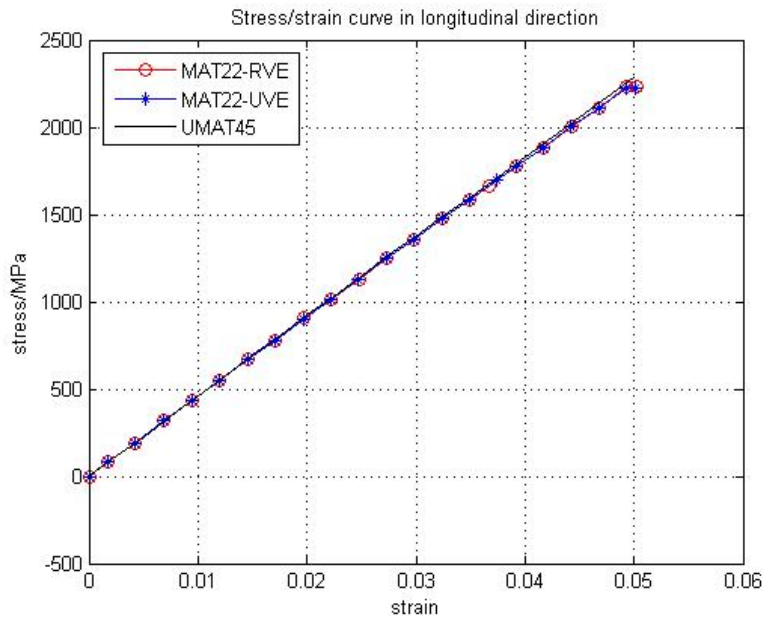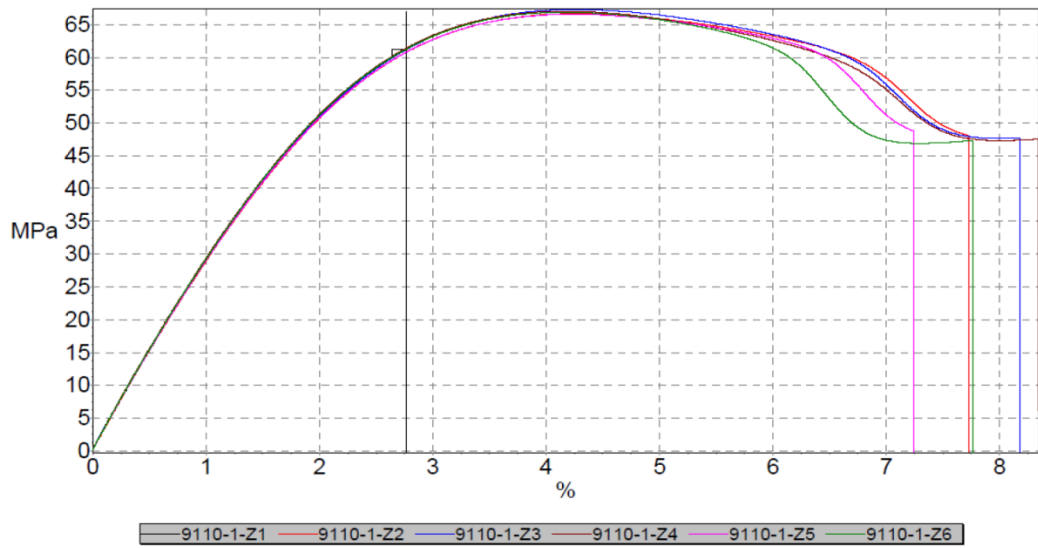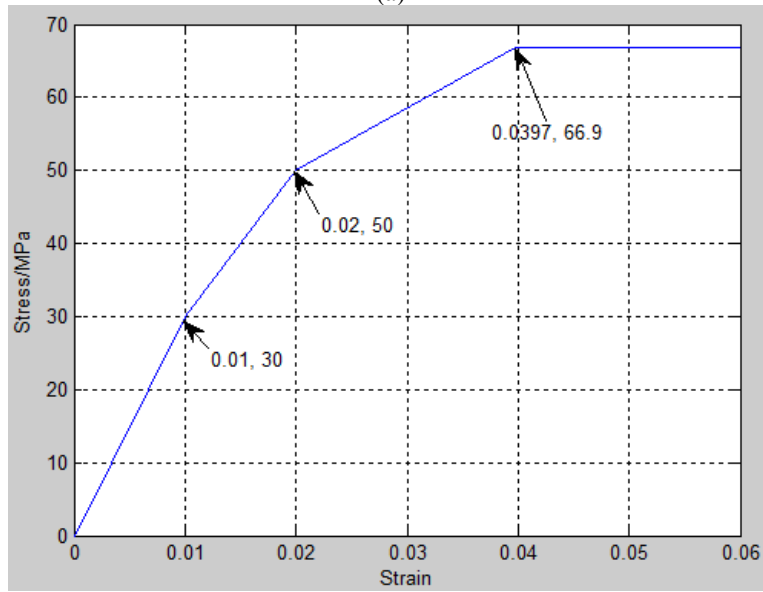
(a)
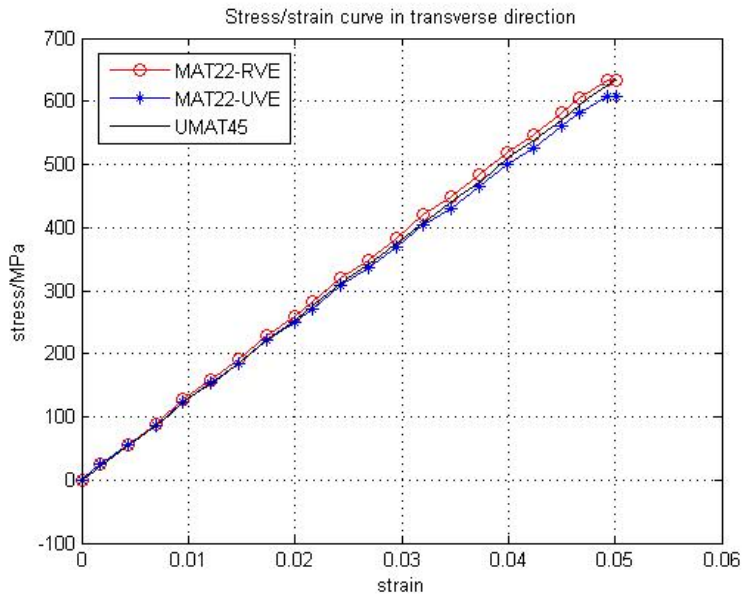
(b)

Figure 13. Comparison of material behavior in elastic case from single element tensile test in (a) longitudinal direction and (b) transverse direction
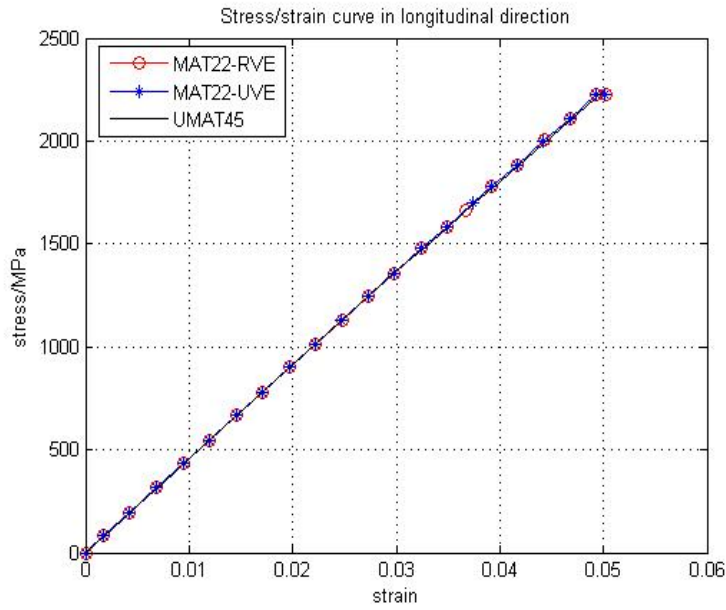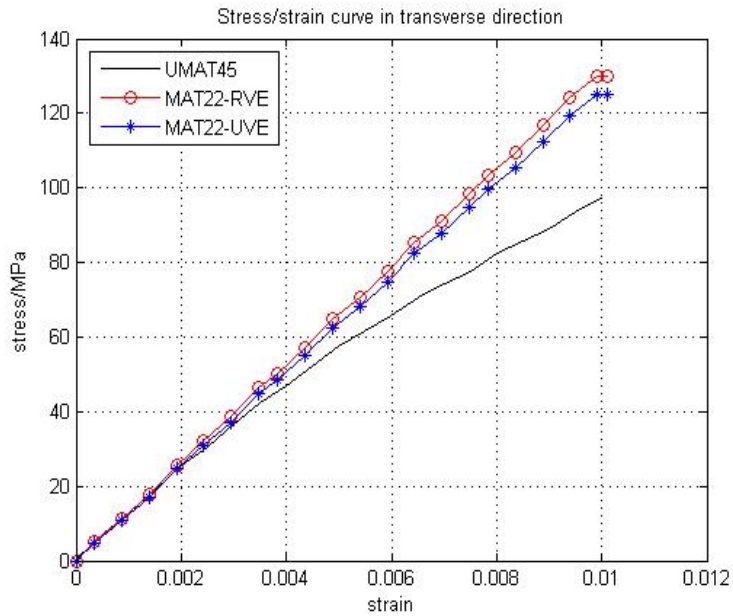
(a)

(10)

Figure 14. Stress/strain curve of epoxy from (a) tensile test and (b) approximate behavior to be implemented in Abaqus

(a)

(b)

Figure 15. Comparison of material behavior in elastoplatic case from single element tensile test in (a) longitudinal direction and (b) transverse direction

SUMMARY AND DISCUSSION

In this paper, a framework of multi-scale modeling of composites under high strain rate impact is proposed to overcome the huge computational burden coming with typical multi-scale modeling technique and make the uncertainty analysis through numerous repetition a practical option. Single element tensile tests, both elastic and elastoplastic, are done to verify the surrogate based material model.

More numerical examples, which consider interfacial debonding and fiber fracture, will be studied to provide further verification. And experiments will be conducted in the future to validate the proposed integration scheme for multi-scale modeling.

REFERENCES

1. Kanouté P, Boso DP, Chaboche JL, and Schrefler BA (2009) Multiscale methods for composites: a review. Arch. Comput. Methods Eng.16: 31–75.
2. E W, Engquist B, Li XT, Ren WQ, and Vanden-Eijnden E (2007) Heterogeneous multiscale methods: a review. Commun. Comput. Phys. 2: 367–450.
3. Eshelby JD (1957) The determination of the field of an ellipsoidal inclusion and related problems. Proc. R. Soc. Lond. A 241: 376-396.
4. Hashin Z (1962) The elastic moduli of heterogeneous materials. J. Appl. Mech. 29: 143-150.
5. Mori T, Tanaka K (1973) Average stress in the matrix and average elastic energy of materials with misfitting inclusions. Acta Metall. 21: 571-574.
6. Kim J (2011) Homogenization and uncertainty analysis for fiber reinforced composites. PhD thesis, University of Florida, Gainesville, F.L.
7. Zhou YX, Jiang DZ, and Xia YM (2001) Tensile mechanical behavior of T300 and M40J fiber bundles at different strain rate. J. Mater. Sci. 36: 919-922.
8. Chi ZF, Zhou TW, and Shen G (1984) Determination of single fiber strength distribution from fiber bundle testing. J. Mater. Sci. 19: 3319–3324.
9. XIA YM, YUAN JM, and YANG BC (1994) A statistical model and experimental study of the strain-rate dependence of the strength of fibers. Compos. Sci. Technol. 52: 499–504.
10. Zhou YX, Jiang DZ, and Xia YM (2001) Tensile mechanical behavior of T300 and M40J fiber bundles at different strain rate. J. Mater. Sci. 36: 919-922.
11. Goldberg RK, Roberts GD, and Gilat A (2005) Implementation of an associative flow rule including hydrostatic stress effects into the high strain rate deformation analysis of polymer matrix composites. J. Aerosp. Eng. 18: 18-27.
12. Sacks J, Welch WJ, Mitchell TJ, and Wynn HP (1989) Design and analysis of computer experiments. Statistical Science, Vol. 4, No. 4: 409-435.
13. McKay MD, Conover WJ, and Beckman RJ (1979) A comparison of three methods for selecting values of input variables in the analysis of output from a computer code. Technometrics, Vol. 21, No. 2: 239-245.
14. Lophaven SN, Nielsen HB, and Søndergaard J (2002) DACE A Matlab Kriging Toolbox.